Spike Field Coherence Reveals Complex Cortical Interaction in Human Visual Memory Task

Stephan Grzelkowski[1], Jiye Kim[2] and Gabriel Kreiman[2]

[1]Universiteit van Amsterdam, Master Program Biomedical Sciences, Track Cognitive Neurobiology and Clinical Neurophysiology, Amsterdam
[2]Harvard Medical School, Center for Brain Science, Boston MA

ABSTRACT

Memory formation is an integral aspect of understanding human cognition. Although previously the hippocampus was indicated as the central hub of memory, in recent years, research has shown that neocortical interactions are also involved. Theta oscillations have been indicated as a possible mechanism for sensory integration, facilitating the formation and recall of memor. In this study, we examined the interaction between spikes and the theta-band (3-8Hz) in the Local Field Potential (LFP), both in the surrounding LFP and in the LFP signal from distant areas, in a Mooney image recognition task in human epilepsy patients with implanted micro-wires. We found that there are few areas that show a difference in Spike Field Coherence (SFC) between novel and recognized Mooney images, for interactions of spikes and the theta band within one recorded channel. However, when examining modulation of firing pattern with theta rhythms of distant regions, we revealed complex interactions in a wide range of cortical areas. Surprisingly, the parahippocampal gyri and the occipital lobe are affected most strongly in a distinction between novel and recognized trials, rather than the hippocampus as previously expected. Our results indicate that a wide range of cortical areas play an important role in memory formation. Furthermore, we provide more evidence for the hypothesis, that the theta frequency band provides a mechanism for information transfer between neuronal circuits.

INTRODUCTION

Theta oscillations (3-8Hz) in the hippocampus are a widely reported phenomenon of the local field potential (LFP) of intracranial recordings[1,2]. They are a prominent feature of the hippocampus during memory task engagement in rodents[3] and humans[4,5]. The theta frequency band of the hippocampal LFP is functionally linked, among other things, to spatial navigation in rodents, and humans in virtual environments[6] and real-world movement[7]. Although most of the research on the theta frequency band has been focused on the hippocampus, other cortical areas such as the occipital, temporal, and parietal lobes, also show increased theta power during nonspatial working memory tasks[8,9].

A large portion of neurons in different structures of the brain are driven by theta rhythms. Single neuron activity is modulated by the theta oscillation, most prominently in the hippocampus, where a large portion of neurons show preference for a specific phase of the theta cycle[10,11]. This phase-dependent firing of neurons across the brain is involved with different tasks[12]. The theta-phase-specific firing of hippocampal cells is shown to be an important component of spatial navigation tasks in rodents, known as phase precession[13]. Theta-locked V1 neurons of the visual cortex show elevated firing rates during their preferred theta phase, when holding information about a visual stimulus in working memory[14]. During periods of reward expectancy orbitofrontal neurons in the rat brain, also showed significant locking to the ongoing theta-oscillations[15]. Shifts in preferred phase, reveal a more nuanced feature of the interaction between spikes and LFP signals. Hippocampal neurons show a preference for the trough of the theta oscillation when the rat is engaged in the memory formation component of a task as compared to a preference for the peak when engaging in memory recall[16]. Siegele and Wilson[17] showed that phase-specific disruption of the ongoing hippocampal theta oscillation, using optogenetic stimulation in CA1, inhibits task performance. This effect was only elicited if the stimulation coincided with the preferred phase of corresponding task segment.

It has been suggested that the phase dependence of neurons in the brain to specific frequency bands is a crucial mechanism for integration and temporal synchronization of information between different areas of the brain[1,18]. Neurons in a variety of cortical regions synchronize their firing with the hippocampal theta rhythms: During spatial navigation of rodents a significant portion of the neurons in the medial prefrontal areas show phase preference to the hippocampal theta rhythm[10,12,19,20]. O'Keefe et al.[21] found a similar relationship between the hippocampal LFP and entorhinal grid cells. The phenomenon of theta locking is widespread throughout the neo-cortex. However, the complex interactions between spiking behavior and LFP across different areas is still poorly understood.

In this study, we expand previous findings on modulation of firing behavior by the theta frequency band to a large set of cortical areas. We investigated this effect in an object recognition task using novel vs learned stimuli of identical Mooney images. The stimuli consist of pairs of two corresponding images, one being a grayscale scene with a target object to be identified and a second, heavily pixelated, scaled-down black and white image, complementary to a grayscale image depicting common objects. Mooney images are easily recognizable after few exposures to the original grayscale image[22]. We recorded LFP and spike data from human epilepsy patients with the use of micro-wires. The strength of the phase-locking can be quantified using the Spike-Field-Coherence (SFC), which is a measure of the relative power of frequency specific oscillations present in the LFP signal centered around the spikes[23]. High SFC indicates synchrony between spike trains and frequency specific signals within the LFP and has been shown to be a predictor for human memory strength in a working memory task[24].

We report a large portion of all isolated neurons, about 85%, to be significantly phase-locked to the theta rhythm of the surrounding LFP. We do not find changes in preferred phases of recognized vs novel stimuli. However, the different conditions elicit SFC changes in various areas and we report a multitude of interactions between spikes in one and LFP of distant areas, indicated by changes in the SFC. Areas that show the most consistent effects include the occipital lobe and the parahippocampal gyri.

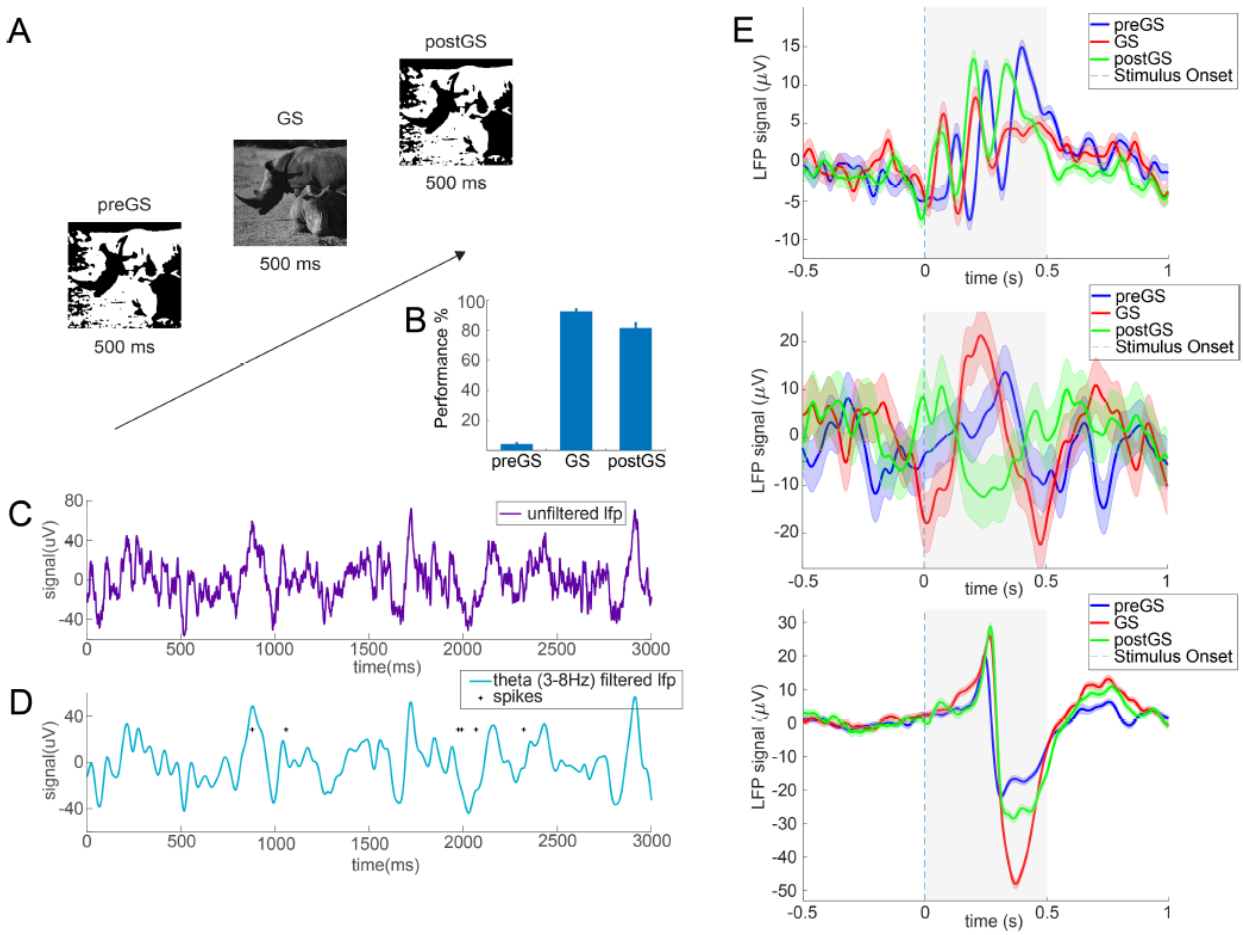

Figure 1 Task Setup and LFP theta band

(A) Example of Mooney and grayscale stimuli presented and the condition nomenclature. Pre-grayscale (preGS) are Mooney images whose respective grayscale pair has not been shown. Stimuli that are shown, after the grayscale (GS) version were presented, are called post grayscale (postGS). **(B)** Recognition performance for the 3 image conditions averaged over patients (n = 14). **(C)** Example trace of a 300Hz lowpass-filtered signal, 3 seconds long. **(D)** Same trace as in (C) but filtered for the 3-8Hz range. Stars denote the spikes that occurred within this segment of the LFP, denoted by '*'. **(E)** Three examples of the Stimulus triggered, theta-filtered (3-8 Hz), LFP in one channel, averaged over all trials of the respective stimulus condition (preGS in green, GS in red, postGS in blue). Shaded Areas denote the Standard Error of the mean. The broken line represents stimulus onset and the gray rectangle denotes the duration of the stimulus presentation. The three channels are located in the occipital lobe, hippocampus and parahippocampus respectively. All channels shown here have a significant difference for the area under the curve (AUC) in the 500ms after stimulus onset ($p < 0.015$, 0.01 false-discovery-rate corrected, between the preGS and postGS condition.)

RESULTS

Theta filtered LFP response to Stimulus Presentation

We presented two different types of stimuli, consisting of pairs of grayscale and Mooney images. The grayscale images depicted common scenes like animals, buildings, and objects. The complementary Mooney image depicted the same scene as the grayscale version thresholded to black and white, resulting in an image difficult identify (***Figure 1A***). Each image pair was presented multiple times in varying succession of Mooney and grayscale image, where each Mooney image was presented at least once before its complementary grayscale image was shown. Mooney images shown before the grayscale version (GS) of that image was shown, are named pre-Grayscale (preGS) and images shown after the grayscale version are named post Grayscale (postGS). The subjects had to indicate knowledge about the scene with a button press and subsequently identify the presented object verbally. Without predisposition to the GS image of the same scene the preGS images were difficult to identify. Both GS and postGS images showed a significant increase in correct identification of trials across patients (t-test, $p < 0.001$) (***Figure 1B***) compared to the preGS conditions. Subjects were epilepsy patients (n = 13) implanted with micro-wire-electrodes in multiple locations across the brain, allowing for simultaneous recordings of the cortical signal in different areas[25]. The experimental setup allowed us to investigate the differences in cortical signaling between novel, unrecognized Mooney images (preGS) and later, recognized repetitions (postGS).

The local field potential is the low frequency (0-300Hz) component of the recorded micro-wire signal. We further filtered the LPF in the 3-8 Hz range using a bandpass Kaiser window filter. To measure the modulation of the theta oscillations between preGS and postGS trials, we calculated the area under curve (AUC) of the filtered signal for two

Location	# signi.	% signi.	Tot. # electrodes
Left Amygdala	1	1.30	77
Right Amygdala	6	8.82	68
Left Entorhinal Cortex	2	7.41	27
Right Entorhinal Cortex	3	18.75	16
Left Hippocampus	2	3.03	66
Right Hippocampus	3	3.75	80
Left Occipital Lobe	10	55.56	18
Right Occipital Lobe	12	31.58	38
Left Parahippocampal Gyrus	16	39.02	41
Right Parahippocampal Gyrus	0	0.00	13
Left Anterior Temporal Lobe	2	8.00	25
Right Anterior Temporal Lobe	1	14.29	7
Left Posterior Temporal Lobe	1	2.00	50
Right Posterior Temporal Lobe	12	28.57	42
Right Parietal Cortex	0	0.00	6

Table 1 Stimulus modulated LFP regions
Shown are the channels in each region that show a significant difference between the LFP response (AUC) in pre and post GS trials in the 500ms window after stimulus onset ($p < 0.0016$, FDR corrected t-test). Prior to analysis all channels that showed a significant difference between the 2 conditions in the Baseline Window ($p < 0.05$, t-test)

different time windows, 500ms before (Base) and 500ms after (Stim) stimulus onset **(Figure 1D)** of trials of both conditions. To eliminate non-task-related effects, all channels that showed a significant difference between the three conditions (ANOVA, $p < 0.05$) in the Base window were not considered further. We performed further analysis between preGS and postGS conditions only, as the feature of interest was the differences in cortical processing of unrecognized versus identical images, rather than differences in stimuli response that might be induced by the different images presented in the GS condition. In order to test the population response to differences in stimuli, we performed t-tests of the AUC of the filtered LFP in the Stim window for each channel separately. To find a reliable p-value threshold that was unaffected by the multiple comparison problem, we calculated the False-Discovery-Rate with an allowance of 0.01 (Methods). A comprehensive list of the portion of significant channels for each area is shown in Table 1.

Areas with the highest percentage of modulated channels include the occipital lobe (55.56% and 31.58%; left and right respectively), the left parahippocampus (39.02%), and the right posterior temporal lobe (28.57%). These areas have been previously indicated to show modulation in human LFP theta band activity during memory task engagement[8,26]. The lack of consistent changes in population activity in the hippocampus is surprising but could indicate that the hippocampal engagement in memory tasks is dependent on specific spike timing rather than changes in the population response.

Phase-locking

To analyze if neurons in different regions were phase-locked to the theta frequency (3-8 Hz), we transformed the LFP signal using MATLAB's complex Morlet wavelet function (*Methods*). This allows us to extract the instantaneous phase at the time of each spike occurrence in a specific frequency band. Figure 2A shows an example of the circular distribution of phase values for a specific frequency of a single neuron. We used the Rayleigh test for non-uniformity around the circle to indicate if the neuronal activity is gated by the phase of an oscillation ($p < 0.0083$, Bonferroni corrected for multiple comparisons; ***Figure 2B***).

In total 1226/1433 (85.5 %) of all neurons were phase-locked to the theta rhythm, a proportion significantly larger than reported in previous human micro-wire recording in the MTL[24]. To see if the proportion of theta-locked neurons varied across sites we looked at neurons of each location separately. We found that 91/132 (68.9%) of neurons in the hippocampus were phase-locked, close to the 80% of phase-locking of neurons that has been reported in the rodent hippocampus[20]. Most areas show a high proportion of neurons to be phase-locked to the theta rhythm, with many areas ranging around 90% phase-locking (for a complete list of phase-locking separated by area see Supplementary Materials 1). Neurons in contralateral areas showed similar proportions of phase-locking, with a mean difference of 12.2% (±13.1 st.dev.). Phase-locking has been previously connected to different functional processes such as spatial navigation and object memory tasks in rodents[13,16,17,21]. Our findings add more information to the relation of neuronal populations in different areas of the brain and theta oscillations.

Same electrode Spike Field Coherence

Next, we were interested in the modulation of the strength of the phase-locking by different conditions, measured in the Spike Field Coherence (SFC). SFC describes the precision of phase-locking of spikes to specific frequencies of the LFP band. It is computed using the frequency spectrum of the spike triggered average (STA) and the average frequency spectrum of all LFP traces, used to compute the STA, and is thereby normalized for the power present in the LFP. SFC takes values from 0-100%.

$$SFC(\omega) = [\frac{fSTA(\omega)}{STP(\omega)}]100\% \quad (1)$$

As previously noted, we only compared the preGS and the postGS conditions. For each neuron we calculated the SFC as the average of all images (using spikes in the 500ms post stimulus window of all repetition) and took the average SFC of frequencies in the theta range (3-8 Hz) (***Figure 2C/D***). We constructed scatter plots, showing the preGS SFC against the postGS SFC for all neurons (***Figure 3B***). Points above the mid-line indicate that the postGS SFC for that neuron is larger than the preGS SFC. We determined whether stimulus condition significantly modulates the SFC by calculating the ratio of neurons above and below the mid-line and estimating the chance of that ratio randomly occurring in randomly assigned groups (permutation tests, n = 1000, methods).

There were no significant areas with significant difference in ratios, except the following two: (1) in the left occipital lobe that showed a larger SFC in the preGS trials as compared the SFC in the postGS trials ($p < 0.001$, permutation test) and (2) the right amygdala, with a slight increase in postGS values ($p < 0.025$, two-sided permutation test). The observed effects due to memory modality may be specific to object recognition in Mooney images. The lack of differences in Spike Field Coherence between novel and recognized stimuli suggest that synchronization of neurons with their immediate surrounding is not an important factor in determining engagement in memory formation or recall.

Inter-regional Spike Field Coherence

To investigate how different forms of task engagement affect inter-area coherence, we performed the same SFC calculation as described in the previous section, using the spikes of one region and the LFP of all other recording sites in the same patient. We expected that integration of information between different structures plays an important role in memory recall and formation[1,17]. As previous research has shown, the locking of spikes in one structure to the ongoing oscillations in another, could be a mechanism that is involved in the transfer of information among them[10,12,20]. Constructing the same scatter plots and performing the same permutation test as described earlier (***Figure 3B/C***), we obtain p-values for all pairs of regions (***Figure 3D***). This figure

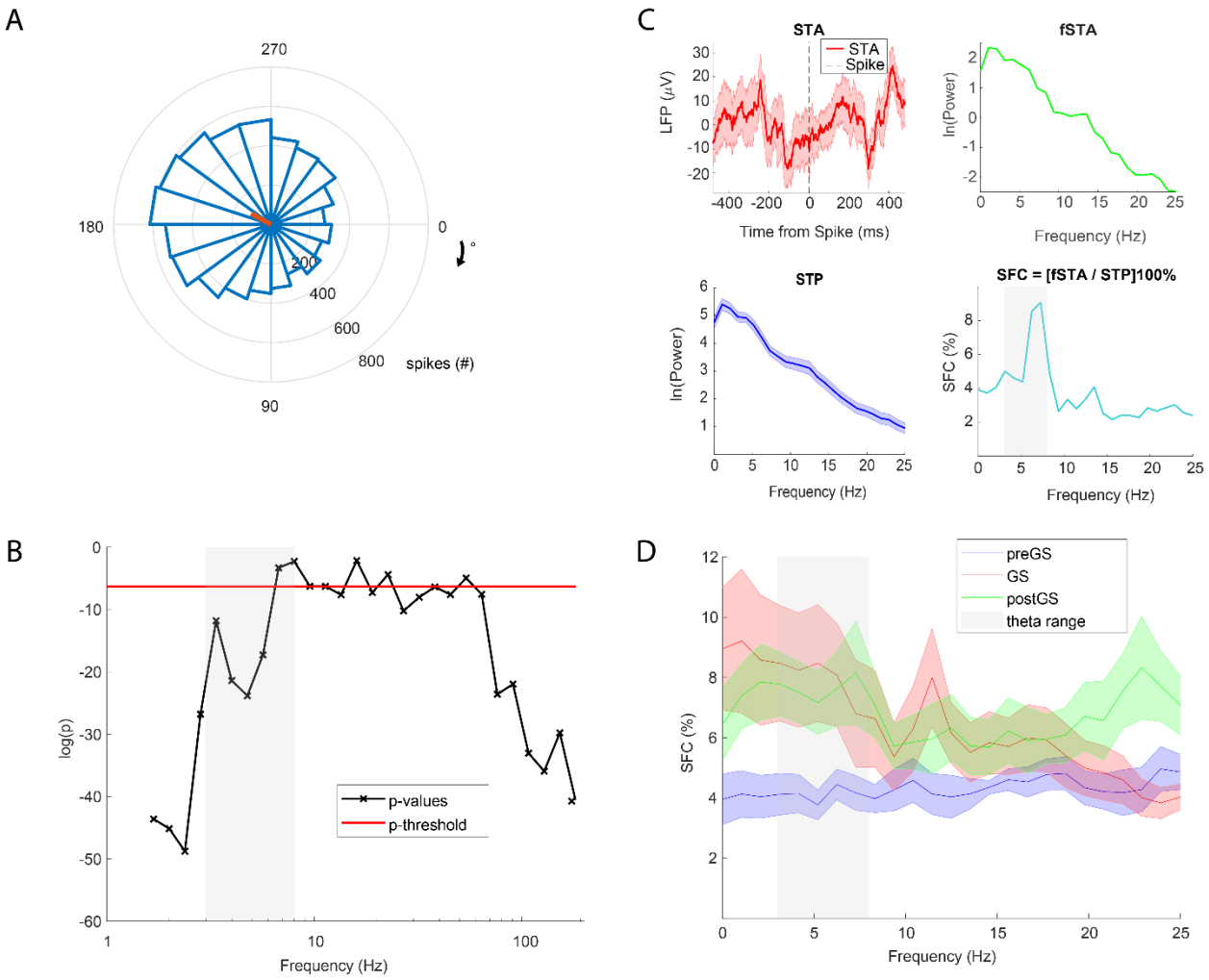

Figure 2 Phase-locking and SFC example

(A) Circular histogram of the phase distribution of an example neuron in the left posterior temporal lobe at the frequency 5.3 Hz. 0 and 360 degree correspond to the trough of the oscillation and 180 degree to the peak. **(B)** Logarithm of the p-values of the Raighley test for non-uniformity of the phase distribution for the frequency range 0 - 180 logarithmically spaced. Red line indicates the p-value threshold corrected for multiple comparison ($p<0.0083$, Bonferroni-corrected, 6 comparisons). A neuron is denoted phase-locked if any of the Raighley tests performed in the 3-8 Hz range cross that threshold. **(C)** Shows the process of calculating the Spike Field Coherence (SFC). First the Spike-Triggered-Average (STA) is constructed using a 960ms time window centered on the spikes. f(STA) is the frequency spectrum of the STA, computed with the Welch's power spectral density estimate. The Spike Triggered Power (STP) is the average over of the LFP traces used to construct the STA, in the same way as the f(STA). The SFC is the quotient of the f(STA) and the STP. The SFC is calculated for each image type and condition separately - using the spikes of all repeated presentations of the same image of one condition. All frequency spectra are calculated for all frequencies in the range 1-481Hz but shown are only the lower ranges. All shaded areas denote the SE. **(D)** SFC of one example neuron averaged over all images presented of one condition, as described in (C). Shaded Areas show SE. The gray rectangle shows the frequency range of interests (3-8Hz).

depicts significant modulation of the SFC in a large variety of regional pairs.

All regions show at least one significant interaction with one other region. The occipital lobe and the parahippocampus were most closely linked to other structures, in that the difference of preGS and postGS Mooney images significantly modulated most of their interactions.

Interestingly the direction of the effect is varied across regions. For example, in the occipital lobe most interactions show an increase in SFC during the preGS trials, whereas interactions of the parahippocampal gyri with other regions show predominantly an increase during the recognized postGS trials. This result suggests that during different modalities of memory, e.g. memory formation during the novel, preGS trials and memory recall or consolidation, during the recognized postGS trials, interaction between areas play different roles.

Although the hippocampus has been widely reported to be generally involved in memory formation and recall[1,17,27], we only find sporadic modulation of the interaction between the hippocampus and other regions by different conditions (**Figure 3D**).

These results suggest that there is a complex network of interactions between different structures involved in the formation and recall of memory. Differences in SFC values between the two conditions show that precise spike timing to the theta rhythms plays an important role.

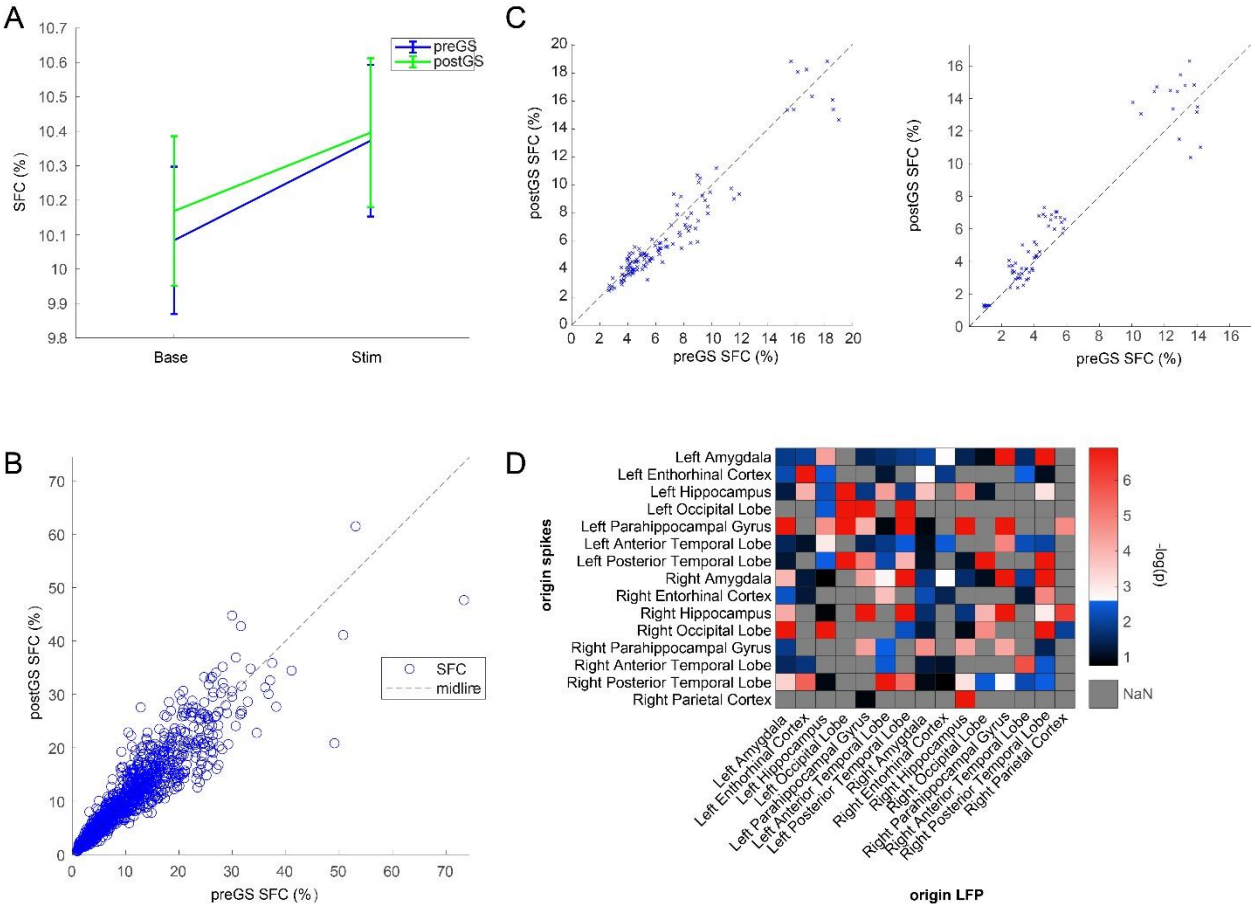

Figure 3 SFC Interaction within and across areas

(A) Shows the average SFC values of all neurons with the LFP in the same electrode. The x-axis denotes the time window of the spikes used. Stim is the 500ms post-stimulus window and Base is the 500ms pre-stimulus window. Different color are show the stimulus condition (preGS vs postGS). 2-way ANOVA did not yield a significant difference between conditions and baseline / stimulus. **(B)** Scatterplots of the average SFC in the theta range, in the post Stimulus window, of all phase-locked neurons, between preGS and postGS. Each point represents one neuron (n = 1204). If the point lies above midline it indicates the neuron has a higher SFC of spikes occurring during postGS trials compared to preGS trials and vice versa. P-values are calculated using permutation tests on the ratio of points above to below the midline. **(C)** Same plot as in (B), but the SFC is calculated with spikes of neurons in one location with the LFP of another. The shown examples are of the LFP in the left occipital (n = 116) and parahippocampal (n = 112) lobes with spikes of neurons in the right and left hippocampus respectively ($p < 0.001$, permutation tests). **(D)** Indicates the p-values of the permutation tests described in (B) on the scatterplots of all SFC interactions with examples given in (C). The redder a square is, the lower the p-value is for that interaction. The y-axis denotes the origin of the spikes and the x-axis denotes the origin of the LFP.

DISCUSSION

Our results provide further evidence that the coherence between spikes and the LFP theta band plays an important role in the encoding and recall of memory in cortical and MTL structures. Although theta-locking is widely present in most areas, the presentation of novel versus learned Mooney images significantly modulated the SFC of neurons to the immediate surrounding in only 2 of the 15 areas. This suggests that the precise timing of the spikes to the theta oscillation in surrounding tissue is not an important factor in either object recognition and memory recall, as those processes best distinguish the trials of novel and recognized Mooney images.

However, we found that presentation of novel and the recognized Mooney images induced modulation in coherence of spikes to the theta rhythm from distant regions. The occipital lobe and the parahippocampus showed consistent changes in the strength of spike timing with most of their paired areas and neurons. Although the occipital lobe is largely seen as a visual processing module, our results indicate a link to memory formation and recall. This is further evidence for the hypothesis, that cortical interactions play an important role in memory formation, as opposed to the idea, that memory processes are confined to the medial temporal lobe (MTL) regions. A connection can be drawn between this example of a visual recognition tasks and the effects found in the visual areas of the occipital lobe. Examining SFC responses in auditory areas during an auditory memory task could provide further insight in the modality of memory formation and could highlight involved neural circuits.

Currently, the synchronization of spike trains to LFP oscillations has unknown origins. It has been shown that projections from different areas of the MTL such as the Ventral Tegmental Area (VTA) and the Locus Coeruleus (LC) drive hippocampal theta rhythm[28–31]; and hippocampus theta rhythms drive spiking activity of neurons in a variety of regions[1,12,20]. However, which cellular mechanisms drive these interactions remains unclear and further research is required to draw definite conclusions on what drives the synchronization of spikes to specific frequency rhythms.

Although there are a wide range of reports on the importance of spike timing to the LFP for memory engagement, it remains difficult to draw clear links to function and behavior, due to the complexity of the interaction. Studies carried out by Siegele & Wilson[17] showed that peak and trough disruption of the theta cycle, using optogenetic stimulation in the hippocampus during memory formation and recall, affects performance of spatial navigation in rodents. Similar studies could investigate if the same effects can be elicited by disrupting different areas.

Spike-timing dependent plasticity (STDP) has long been indicated as a crucial mechanism for sensory integration and memory formation[32]. It remains to be seen if SFC could be a driving factor of facilitating STDP between neuron populations in distant regions.

Our result suggests, that processes of memory formation are not limited to hippocampal-cortical interaction. We have shown, that Spike timing to the theta rhythm is significantly modulated by novel vs recognized identical images in a range of cortical areas and that these effects extent to interregional connections. These findings present a basis upon which future research can built to explore the importance of both spike timing and LFP theta activity for memory formation within different neuronal circuits.

METHODS

Recording, Stimulus presentation

We recorded micro-wire signals from 13 epilepsy patients over 36 sessions, engaged in a Mooney image recognition task. The Stimuli were presented in blocks of 60 images. Each set of images consisted of a Mooney image and a corresponding grayscale image showing the same object. All stimuli were presented for 500ms. The Mooney image was presented first in the pre-grayscale condition (preGS). If The subject recognized the object, they could respond with a button press. In case of a negative response, indicating no recognition, or no button press, the same image was presented again 1300ms after the first one. After multiple repetitions of different Mooney images, the grayscale (GS) version of the same images were shown. Again, the subject could give a response with a button press. After the patient indicated they recognized the object, a prompt showed up asking to report the perceived object. The experimenter marked the response as correct or false. If the response was correct the Mooney image version (postGS) was shown back to back with the GS to reinforce learning. This process was repeated until the Mooney images were correctly classified or until the patient was unable to classify the item 15 times. Trials of the preGS condition, that were recognized by the patient, as well as all trials that were not correctly recognized in the GS and postGS conditions were not considered further.

Spike Sorting

Spike sorting was done in 3 steps. First the signal was band-pass filtered 300-3000Hz and subsequently the signal was notch-filtered for all harmonics of 50 Hz. As a last step the spikes were sorted using the Osort-method described by Rutishauser et al.[33].

Filter and LFP analysis

To obtain the LFP, the signal was low-pass filtered with a cutoff at 300Hz and notch filtered at 50Hz and all its harmonics. To analyze the effects of the different stimuli conditions in a specific frequency band, the signal was again filtered using a band-pass filter on the specified frequency range with a 3rd order Kaiser window. Each electrode was analyzed on differences between the three conditions in the window 500ms before stimulus presentation (Baseline) using the area under curve (AUC). AUC was computed as the integral of the LFP on that time window, formally:

$$P_i = \int_a^b S_i(t)^2 dt \tag{2}$$

Where Si(t) is the filtered LFP signal of trial *i* and *a* and *b* denote the time window relative to stimulus onset. We removed all electrodes from further analysis that showed a significant difference ($p < 0.05$; ANOVA) between the three conditions. After removing trials effected by baseline changes with this method, we compared the stimulus response (AUC) of preGS and postGS trials in the 500ms post stimulus window using a t-test. The p-value threshold was calculated based on the False Discovery Rate (FDR). To calculate the FDR, we performed a random permutation test. We shuffled the labels of the Stimulus conditions randomly for 1000 iterations and computed the t-test p-value for each. Next, we calculated for a range of p-value-thresholds (0.001, 0.002, ... 0.05), how many of the 1000 tests were deemed significant under the selected accepted rate of false discovery ($p < 0.01$). We selected the last p-value that resulted in less than 1% of the t-test showing significance ($p_{FDR} = 0{:}015$)

Phase-Locking to theta-oscillation

All neurons with a firing rate above 0.5Hz were tested for phase-locking to theta range (3-8Hz). The unfiltered LFP was transformed using the complex Morlet wavelet (34) using 28 scales logarithmically spaced between $[2^{\frac{6}{8}}, 2^{\frac{8}{8}}, \ldots, 2^{\frac{60}{8}}]$ resulting in Frequencies ranging from 1.7 - 181 Hz. The wavelet was applied with a bandwidth of 4 and a center frequency of 1. The angles of the resulting complex values associate every time-point of the recording with a specific phase at a specific frequency. To test if a given neuron was phase-locked, phase-values of all spikes were tested on non-uniformity using a Rayleigh-test. A neuron was assigned as phase-locked if for any of the frequencies between 3-8 Hz a p-value showed significance ($p < 0.0083$; Bonferroni corrected, Z-statistic) was reached.

Spike Field Coherence

All theta-locked neurons were included in the analysis for Spike Field Coherence (SFC). SFC is a function of frequency and the number of spikes and indicates the strength of a neuron's preference to fire at a specific phase ρ of a particular frequency ω. Before we computed the SFC, we subsampled the spikes from all the repetitions of one image within a condition, so that each stimulus condition had the same number of spikes. Additionally, we calculated the firing rate during the stimulus presentations of all images and discarded images that had less than 2 spikes in the combined presentations of their repetitions within one condition. We discarded all neurons that met any of the following 2 criteria: (1) if they had a firing rate below 0.5Hz and (2) had less than 5 images with sufficient spikes under the criteria above. The SFC was then computed for each neuron separately as the average of the SFC of each image, using the spikes across all its repetitions. First, the Spike Triggered Average (STA) of the LFP was calculated for 480 ms before to 480 ms after the spike time. This time window was chosen as we are interested in the slow theta oscillations[23,24]. As a next step we calculated the frequency spectrum of the STA (fSTA) and the Spike Triggered Power (STP), which is the average power spectrum of all the LFP traces used to calculate the STA. The fSTA is the power spectrum around the spike, whereas the STP is the average power present in the LFP used to construct the STA. The SFC is the ratio between the two, formally:

$$SFC(\omega) = [\frac{fSTA(\omega)}{STP(\omega)}]100\% \quad (3)$$

for a specific frequency ω. We calculated the average SFC of a specific neuron for each condition separately.

Scatter Plots, permutation tests

To see how separate neurons react to different stimulus conditions, we plotted each neuron on a scatter plot where each of the axes is the average SFC in a specific condition. If a neuron was indifferent to conditions, it was expected to lie close to the mid-line. We were interested in what proportion of the neurons showed a preference in SFC for one of the conditions. Permutation tests gave an approximation of the chance of the observed effect appearing randomly. First, we calculated the ratio between points above the mid-line to points below the mid-line. We took the number of neurons used to create the scatter plot and simulated for 1000 iterations a new distribution of ratios between points above and below mid-line, by randomly assigning a neuron to the condition above or below.

$$r = \frac{n_{above} - n_{below}}{n_{total}} \quad (4)$$

The p-value of the original ratio was calculated as the portion of simulated ratios that were more extreme.

$$p(r) = \begin{cases} \frac{[r^* > r]_\#}{n}; & \text{for } r > 0 \\ \frac{[r^* < r]_\#}{n}; & \text{for } r < 0 \end{cases} \quad (5)$$

where n is the number of iterations and [:::]# indicates the number of cases for which the expression inside the brackets is true. This gives the approximate probability to find the observed ratio by chance.

REFERENCES

1. Buzsáki, G. Theta Oscillations in the Hippocampus. *Neuron* **33**, 325–340 (2002).

2. Mormann, F. Independent delta/theta rhythms in the human hippocampus and entorhinal cortex. *Frontiers in Human Neuroscience* **2** (2008).

3. Lee Colgin, L. Rhythms of the hippocampal network (2016).

4. Arnolds, D., Lopes Da Silva, F., Aitink, J., Kamp, A. & Boeijinga, P. The spectral properties of hippocampal EEG related to behaviour in man. *Electroencephalography and Clinical Neurophysiology* **50**, 324–328 (1980).

5. Lega, B. C., Jacobs, J. & Kahana, M. Human hippocampal theta oscillations and the formation of episodic memories. *Hippocampus* **22**, 748–761 (2012).

6. Kahana, M. J., Sekuler, R., Caplan, J. B., Kirschen, M. & Madsen, J. R. Human theta oscillations exhibit task dependence during virtual maze navigation. *Nature* (1999).

7. M. Aghajan, Z. et al. Theta Oscillations in the Human Medial Temporal Lobe during Real-World Ambulatory Movement. *Current Biology* **27**, 3743–3751 (2017).

8. Raghavachari, S. et al. Gating of Human Theta Oscillations by a Working Memory Task. *Tech. Rep.* (2001).

9. Jacobs, J., Kahana, M. J., Ekstrom, A. D. & Fried, I. Brain Oscillations Control Timing of Single-Neuron Activity in Humans (2007).

10. Jones, M. W. & Wilson, M. A. Theta Rhythms Coordinate Hippocampal–Prefrontal Interactions in a Spatial Memory Task. *PLoS Biology* **3**, e402 (2005).

11. Fox, S., Wolfson, S. & Ranck, J. Hippocampal theta rhythm and the firing of neurons in walking and urethane anesthetized rats. *Experimental Brain Research* **62**, 495–508 (1986).

12. Sirota, A. et al. Entrainment of Neocortical Neurons and Gamma Oscillations by the Hippocampal Theta Rhythm. *Neuron* **60**, 683–697 (2008).

13. O'Keefe, J. & Recce, M. L. Phase relationship between hippocampal place units and the EEG theta rhythm. *Hippocampus* **3**, 317–330 (1993).

14. Lee, H., Simpson, G. V., Logothetis, N. K. & Rainer, G. Phase Locking of Single Neuron Activity to Theta Oscillations during Working Memory in Monkey Extrastriate Visual Cortex. *Neuron* **45**, 147–156 (2005).

15. van Wingerden, M., Vinck, M., Lankelma, J. & Pennartz, C. M. A. Theta-Band Phase Locking of Orbitofrontal Neurons during Reward Expectancy. *Journal of Neuroscience* (2010).

16. Hasselmo, M. E., Bodelón, C. & Wyble, B. P. A Proposed Function for Hippocampal Theta Rhythm: Separate Phases of Encoding and Retrieval Enhance Reversal of Prior Learning. *Neural Computation* **14**, 793–817 (2002).

17. Siegle, J. H. & Wilson, M. A. Enhancement of encoding and retrieval functions through theta phase-specific manipulation of hippocampus. *elife,* **3**, 3061 (2014).

18. Colgin, L. L. Mechanisms and Functions of Theta Rhythms. *Annual Review of Neuroscience* 36, 295–312 (2013).

19. Hasselmo, M. E. What is the Function of Hippocampal Theta Rhythm? - Linking Behavioral Data to Phasic Properties of Field Potential and Unit Recording Data. *Hippocampus* **15,** (2005)

20. Siapas, A. G., Lubenov, E. V. & Wilson, M. A. Prefrontal Phase Locking to Hippocampal Theta Oscillations. *Neuron* **46**, 141–151 (2005).

21. O'Keefe, J. & Burgess, N. Dual phase and rate coding in hippocampal place cells: Theoretical significance and relationship to entorhinal grid cells, *Hippocampus,* (2005).

22. Mooney, C. M. Closure with negative after-images under flickering light. *Canadian Journal of Psychology/Revue canadienne de psychologie* **10**, 191–199 (1956).

23. Fries, P., Roelfsema, P. R., Engel, A. K., Ko¨nig, P. K. & Singer, W. Synchronization of oscillatory responses in visual cortex correlates with perception in interocular rivalry. *Tech. Rep.* (1997).

24. Rutishauser, U., Ross, I. B., Mamelak, A. N. & Schuman, E. M. Human memory strength is predicted by theta-

frequency phase-locking of single neurons. *Nature* **464**, 903–907 (2010).

25. Ojemann, G., Mamelak, A., Staba, R., Fields, T. & Behnke, E. Single neuron studies of the human brain: probing cognition, *Journal of Neuropathology & Experimental Neurology*, **74**, 1039 (2014).

26. Raghavachari, S. et al. Theta Oscillations in Human Cortex During a Working-Memory Task: Evidence for Local Generators. *J Neurophysiology* **95**, 1630–1638 (2006).

27. Lega, B., Burke, J., Jacobs, J. & Kahana, M. J. Slow-Theta-to-Gamma Phase–Amplitude Coupling in Human Hippocampus Supports the Formation of New Episodic Memories. *Cerebral Cortex* **26**, 268–278 (2016).

28. Orzeł-Gryglewska, J., Jurkowlaniec, E. & Trojniar, W. Microinjection of procaine and electrolytic lesion in the ventral tegmental area suppresses hippocampal theta rhythm in urethaneanesthetized rats. *Brain Research Bulletin* **68**, 295–309 (2006).

29. Bland, B. H. & Oddie, S. D. Theta band oscillation and synchrony in the hippocampal formation and associated structures: the case for its role in sensorimotor integration. *Behavioural Brain Research* **127**, 119–136 (2001).

30. Remondes, M. & Wilson, M. A. Cingulate-Hippocampus Coherence and Trajectory Coding in a Sequential Choice Task. *Neuron* **80**, 1277–1289 (2013).

31. Brown, R. A. M., Walling, S. G., Milway, J. S. & Harley, C. W. Locus Ceruleus Activation Suppresses Feedforward Interneurons and Reduces-Electroencephalogram Frequencies While It Enhances Frequencies in Rat Dentate Gyrus, *Journal of Neuroscience*, **25**, 8 (2005).

32. Dan, Y. & Poo, M.-m. Spike Timing-Dependent Plasticity of Neural Circuits. *Neuron* **44**, 23–30 (2004).

33. Rutishauser, U., Schuman, E. M. & Mamelak, A. N. Online detection and sorting of extracellularly recorded action potentials in human medial temporal lobe recordings, in vivo. *Journal of Neuroscience Methods* (2006).

34. Le Van Quyen, M. et al. Comparison of Hilbert transform and wavelet methods for the analysis of neuronal synchrony. *Journal of Neuroscience Methods* **111**, 83–98 (2001).

Location	# neurons phase-locked	tot # neurons recorded	% phase-locked neurons
Left Amygdala	110	123	89,43
Right Amygdala	201	214	93,93
Left Entorhinal Cortex	32	32	100
Right Entorhinal Cortex	11	17	64,71
Left Hippocampus	91	132	68,94
Right Hippocampus	151	213	70,89
Left Occipital Lobe	28	42	66,67
Right Occipital Lobe	113	122	92,62
Left Parahippocampal GYrus	173	181	95,58
Right Parahippocampal Gyrus	31	34	91,18
Left Anterior Temporal Lobe	75	78	96,15
Right Anterior Temporal Lobe	13	14	92,86
Left Posterior Temporal Lobe	128	138	92,75
Right Posterior Temporal Lobe	66	80	82,50
Right Parietal Cortex	3	13	23,08
Total # of neurons	1226	1433	85,55

Supplemental Material 1 Phase-locking separated by region

Number of neurons that show significant phase-locking by the Raighley-test of non-uniformity ($p < 0.0083$, Z-statistic, Bonferroni corrected for multiple comparisons) for each region separately.